学位論文

The effect of zoledronic acid and denosumab on the mandible and other bones: a ^{18}F-NaF-PET study

伏見 麻央

Oral Radiology
https://doi.org/10.1007/s11282-022-00594-2

ORIGINAL ARTICLE

The effect of zoledronic acid and denosumab on the mandible and other bones: a ^{18}F-NaF-PET study

Mao Fushimi[1] · Yumiko Ohbayashi[1] · Fumi Nakai[1] · Takashi Norikane[2] · Yuka Yamamoto[2] · Yoshihiro Nishiyama[2] · Minoru Miyake[1]

Received: 29 September 2021 / Accepted: 21 January 2022

Abstract

Objectives The primary purpose of this study was to determine whether both zoledronic acid (ZA) and denosumab (Dmab) equally suppress bone remodeling of the normal mandible, and the secondary purpose was to determine the influence of ZA and Dmab on other normal bones.

Methods ^{18}F-sodium fluoride-positron-emission-tomography (^{18}F-NaF-PET) was used to perform quantitative analysis of the bone metabolism in various parts. The end points of the study were the mean standardized uptake value (SUV) of each member of the ZA group ($n=9$), the Dmab group ($n=16$), and the Control group ($n=23$).

Results The SUV at the thoracic vertebrae in the ZA group were significantly lower than those of the Dmab and Control group ($p<0.05$) In addition, the mean SUVs of the cervical vertebrae in the ZA group were significantly lower than those in the Control group ($p<0.05$). There was no significant difference among ZA, Dmab and Control group in the other sites. There was no significant difference between the Dmab and Control groups at all sites.

Conclusions The remodeling of mandible was not suppressed due to the treatment with anti-resorptive agents. Differences in the mechanisms of action between the BP and Dmab caused the specificity of the effect on the metabolism of normal bone.

Keywords Osteonecrosis of jaw · Bone metabolism · Bisphosphonate · Denosumab · ^{18}F-NaF-PET

Introduction

Bone is a common site of metastasis in cancer. Cancer cells can easily settle in bone, and cancer cells that have metastasized to bone undergo secondary multiple metastases starting from bone. The incidence of bone metastases is reported to be 65–95% in breast cancer, prostate cancer, and myeloma [1]. Bone destruction occurs when cancer metastasizes to bone, resulting in skeletal-related events (SREs) such as pathological fractures and hypercalcemia [1]. Many bone pain sensations may also develop, and the proliferation of cancer induces strong bone pain [2]. The reported median survival of patients with bone metastases of breast cancer is approx. 20 months, and that for bone metastases of small-cell lung cancer is 3–6 months [3, 4].

Bone resorption inhibitors such as bisphosphonates (BPs), which are the standard treatment for bone metastasis [5], and denosumab (Dmab), which is a human monoclonal antibody that inhibits the receptor activator of NF-kappaβligand (RANKL), are used for bone metastasis. The rare and very serious side effects of bone resorption inhibitors include atypical femoral fractures (AFFs) and medication-related osteonecrosis of the jaw (MRONJ) [6–8]. The reported incidence of antiresorptive agent-related osteonecrosis of the jaw treated by an oncology dose, i.e., a high dose of a BP (HBP), is 0.4–2.3% [9] and that of cases treated with Dmab is 0.5–3.2% [10]. These levels are similar to the incidence of MRONJ. The incidence of AFF treated with an HBP is 0.4–1.2% [11], and that of AFF treated with Dmab is 1.8% [9]. The mechanisms of AFF and MRONJ remain to be clarified, although both have a common feature in that they inhibit bone remodeling [7, 12]. Bone resorption inhibitor-related osteonecrosis of the jaw is considered to be one

✉ Minoru Miyake
miyake.minoru@kagawa-u.ac.jp

[1] Department of Oral and Maxillofacial Surgery, Faculty of Medicine, Kagawa University, 1750-1 Ikenobe, Miki-cho, Kita-gun, Kagawa 761-0793, Japan

[2] Department of Radiology, Faculty of Medicine, Kagawa University, 1750-1 Ikenobe, Miki-cho, Kita-gun, Kagawa 761-0793, Japan

Published online: 10 February 2022

of the causes of the site-specific effects of bone resorption inhibitors on bone metabolism [13].

Due to the difference in developmental bone formation between long bones and jaw bones, the jaw bones have a higher rate of bone turnover than other bones, resulting in more BP deposition and increased bone uptake in animals [14]. Chang et al. reported that in rats, cells in the craniofacial skeleton are more susceptible to the bisphosphonate zoledronic acid (ZA) compared to cells in the ilium and tibia [14]. Our knowledge about the distribution of BP and Dmab to bone in humans is still limited.

In Japan, a nuclear medicine test using ^{99m}Tc bone scintigraphy is the standard method of assessing bone lesions, whereas ^{18}F-NaF-PET (positron emission tomography) containing ^{18}F-fluoride as an active ingredient is also performed worldwide. The clinical use of ^{18}F-fluoride as a bone imaging agent was initially demonstrated by Blau et al. [15], and it was approved by the U.S. Food and Drug Administration (FDA) as a PET tracer in 1972. ^{18}F-fluoride ions exchange with hydroxyl groups in the hydroxyapatite at the surface of bone crystals, forming fluoroapatite mainly at sites of bone remodeling with high turnover. The uptake of ^{18}F-fluoride thus reflects blood flow and osteoblastic activity.

The bone uptake of ^{18}F-fluoride is twofold greater than that of ^{99m}Tc-MDP (methyl diphosphonate) [16, 17]. Compared with conventional bone scintigraphy, ^{18}F-NaF-PET has the advantage of a shorter examination time, better spatial resolution, and better image quality, which improve the sensitivity and specificity. Compared to bone scans, ^{18}F-NaF-PET can more accurately assess responses to treatment and detect potential bone metastases [18, 19]. Moreover, ^{18}F-NaF-PET results can be quantitatively evaluated by standardized uptake value (SUV) measurements. Its use also makes it possible to discover minute bone accumulations that cannot be revealed by bone scintigraphy.

MRONJ develops only in the jaw, and AFF occurs only in the femur. We hypothesized that both the jaw and femur may have their bone metabolism suppressed equally by BP and Dmab treatment. To test this hypothesis, we used ^{18}F-NaF-PET to perform a quantitative analysis of the bone metabolism at various sites, including the jaw and femur. The primary purpose of this study was to determine whether ZA and Dmab equally suppress bone remodeling of the normal mandible. A secondary purpose was to determine the effects of ZA and Dmab on other healthy bones.

Patients and methods

Study design

This was a matched, case–control study. We compared bone metabolic differences in normal bone between patients who had been administered ZA (the ZA group), patients administered Dmab (the Dmab group), and patients not treated with an antiresorptive agent (the Control group) by conducting a quantitative analysis of ^{18}F-NaF-PET findings. We set the end points of the study as the mean SUV of each of these three groups.

Patients

We analyzed the data of the patients who underwent treatment for bone metastasis at our University during the period from April 2016 to April 2020. The patients' eligibility was based on fulfilling the following criteria: $\geq$ 50 years old and no history of treatment with radiation therapy. The exclusion criteria were as follows: the presence of systemic bone disease (such as osteoporosis or chondrodysplasia), and prior treatment with both ZA and Dmab. The median administration period of the ZA group was 48 months, and that of the Dmab group was 28 months. The ZA group was nine patients (two males and seven females), and the Dmab group was 16 patients (11 males and five females). The Control group was 23 patients (20 males and three females) who had been diagnosed with oral disease or the possibility of bone metastasis. The Control group was drawn from the same period as the ZA and Dmab groups. All patients had undergone an examination by ^{18}F-NaF-PET due to the presence of osteonecrosis or a related condition (Table 1).

^{18}F-NaF-PET

We used the patients' ^{18}F-NaF-PET images for the quantification of the bone uptake of radiopharmaceuticals. All acquisitions were performed using a Biograph mCT 64-slice positron emission tomography/computed tomography (PET/CT) scanner (Siemens Medical Solutions USA, Knoxville, TN). This scanner has an axial field of view of 21.6 cm. Patients need no special preparations to undergo the ^{18}F-NaF PET/CT scan. The data acquisition began with the CT at the following settings: no contrast agent, 120 kV, quality reference milliamperes (mAs), 50 mAs (using CARE Dose4D; Siemens), 0.5-s tube rotation time, 2-mm slice thickness, 2-mm increments, and pitch 0.8. The PET emission scanning of neck spot imaging (10 min per bed position) was performed 60 min after a single intravenous injection of ^{18}F-NaF (approx. 5 MBq/kg). After the neck spot imaging, whole-body PET data from the neck to the mid-thigh level were acquired for 2 min per bed position (5–7 beds). The PET data were acquired in 3D mode and were reconstructed using the baseline ordered-subsets expectation maximization bases, incorporating correction with a point spread function and time-of-flight model (two iterations and 21 subsets; matrix size 256×256).

Table 1 The patients' characteristics ($n=48$)

	Sex	Median age, years	Underlying disease	Median duration of administration, months
ZA group, $n=9$	M: 2 F: 7	74.0	Breast cancer: 5 Prostate cancer: 2 Lung cancer: 1 Multiple myeloma: 1	48.0
Dmab group, $n=16$	M: 11 F: 5	69.5	Breast cancer: 3 Prostate cancer: 8 Lung cancer: 3 Multiple myeloma: 1 Thyroid cancer: 1	28.0
Control group, $n=23$	M: 20 F: 3	71.0	Osteomyelitis: 5 Prostate cancer: 10 Oral carcinoma: 4 Other: 4	—

Dmab denosumab, *ZA* zoledronic acid

The region of interest (ROI) was selected by identifying the area with no abnormal accumulation of the mandibular angle, mandibular ramus, mandibular condyle, body of mandible, cervical vertebrae, thoracic vertebrae, sternum, rib, humerus, iliac crest, second lumbar vertebra, femoral head, and diaphyseal thigh bone (Fig. 1). The identification of the area without abnormal accumulation was performed by two subspecialty nuclear medicine physicians (Y.Y. and Y.N.), and the attending physician in each case confirmed that there were no clinical signs of metastasis or inflammation. Two subspecialty oral surgeons (M.F. and Y.O.) selected the ROIs at sites without active dental disease, osteomyelitis, or clinical or imaging abnormalities. Two observers (M.F. and Y.O) independently analyzed all of the ^{18}F-NaF-PET images to test both inter- and intra-observer variability.

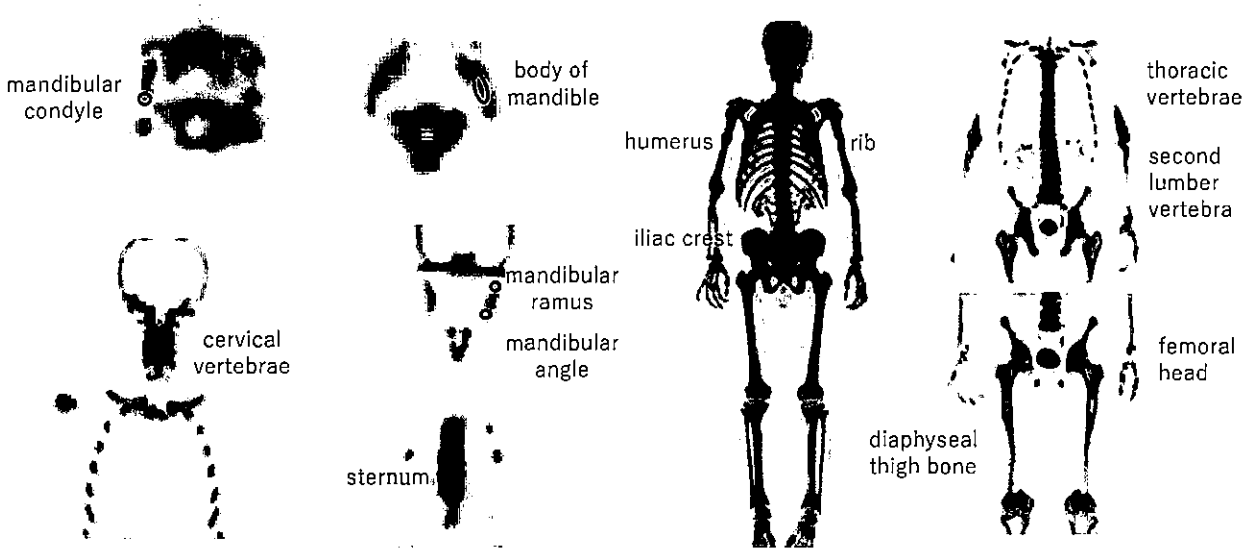

Fig. 1 ROI was selected at the intact region of the each area. *ROI* region of interest

SUV calculation method

The formula for determining the SUV was as follows:

SUV = radiation concentration (Bq/ml)/
dose at the beginning of the scan (Bq)/
body weight (g).

Statistical analysis

We compared the mean SUVs of each bone ROI among the ZA, Dmab, and Control groups. The Kruskal–Wallis test followed by Dunn's test was performed to compare the mean SUVs of the groups. The significance level was set at $p < 0.05$. We determined the inter-observer and intra-observer reliability of each mean SUV measurement by obtaining the intraclass correlation coefficient (ICC). A two-way random effect model was used for inter-observer reliability, and a one-way random effect model was used for the intra-observer reliability. All analyses were carried out using SPSS 25.0 for Windows (SPSS, Chicago, IL).

Results

The median ages were 74.0 ± 8.22 years in the ZA group, 69.5 ± 10.8 years in the Dmab group, and 71.0 years ± 8.28 years in the Control group ($p = 0.449$). The mean SUVs of the ROIs at the thoracic vertebrae in the ZA group were significantly lower than those of the Dmab and Control groups (mean SUV: 4.48, 5.71, and 6.01, respectively; $p = 0.050$, $p = 0.029$) (Table 2, Fig. 2). The mean SUVs of the thoracic vertebrae in the Dmab and Control group were not significantly different. In contrast, the mean SUV of the cervical vertebrae in the ZA group were significantly lower than that in the Control group (4.44 vs. 5.76, respectively; $p = 0.034$). The mean SUVs of the cervical vertebrae were not significantly between the ZA and Dmab groups, or between the Dmab and Control groups.

There was no significant differences among the ZA, Dmab, and Control groups in the mandibular angle, mandibular ramus, mandibular condyle, body of the mandible, sternum, rib, humerus, iliac crest, second lumbar vertebra, femoral head, or diaphyseal thigh bone. No significant

Table 2 SUVmean values in the ZA, Dmab, and Control groups and ICCs

Variable	ZA	Dmab	Control	*p* value	ZA vs. Dmab	ZA vs. Control	Dmab vs. Control	ICC of inter-observer analysis	ICC of intra-observer analysis
Mandibular angle	1.47	1.43	1.41	0.890				0.748 (0.619–0.837)	0.922 (0.866–0.956)
Mandibular ramus	1.33	1.35	1.25	0.775				0.949 (0.915–0.969)	0.869 (0.778–0.925)
Mandibular condyle	1.27	1.37	2.29	0.080				0.870 (0.791–0.920)	0.886 (0.807–0.935)
Body of mandible	2.09	1.84	2.06	0.260				0.947 (0.913–0.967)	0.968 (0.944–0.982)
Cervical vertebrae	4.44	5.45	5.76	0.040*	0.095	0.011‡	0.344	0.911 (0.853–0.946)	0.962 (0.933–0.979)
Thoracic vertebrae	4.48	5.71	6.01	0.024*	0.050‡	0.029‡	1.000	0.892 (0.831–0.932)	0.946 (0.906–0969)
Sternum	3.40	3.34	4.47	0.086				0.921 (0.876–0.951)	0.979 (0.964–0.988)
Rib	1.36	1.76	2.62	0.043*	1.000	0.066	0.248	0.751 (0.601–0.846)	0.904 (0.835–0.945)
Humerus	1.86	1.86	2.06	0.652				0.878 (0.810–0.922)	0.953 (0.918–0.973)
Iliac crest	3.70	4.42	4.30	0.418				0.780 (0.637–0.866)	0.967 (0.943–0.982)
Second lumber vertebrae	4.19	5.19	5.76	0.097				0.761 (0.637–0.847)	0.937 (0.889–0.965)
Femoral head	2.57	2.50	2.44	0.286				0.927 (0.883–0.955)	0.987 (0.976–0.993)
Diaphyseal thigh bone	2.19	2.85	2.28	0.128				0.866 (0.789–0.917)	0.973 (0.951–0.985)

ICC data are followed by 95% confidence interval in parentheses

Kruskal–Wallis test, *‡$p < 0.05$ pairwise comparison by Dunn's test

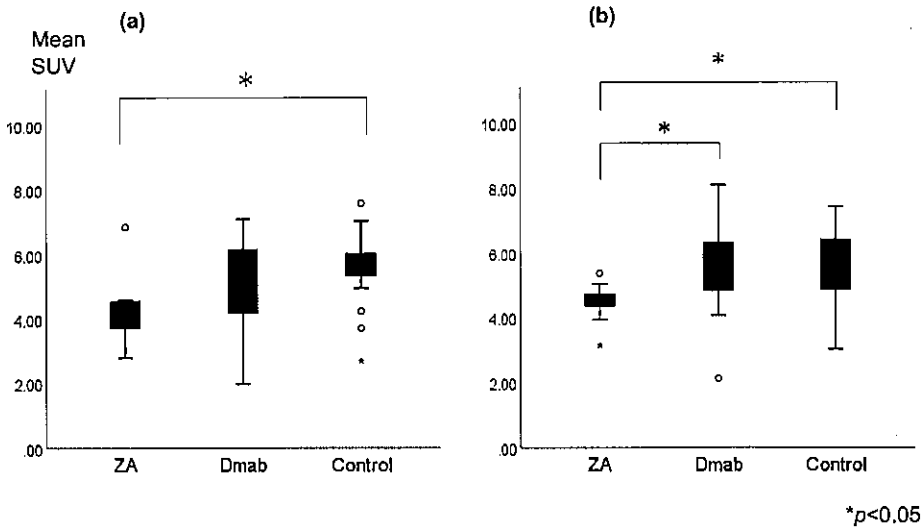

Fig. 2 Mean SUV of cervical vertebrae and thoracic vertebrae. *SUV* standardized uptake value, *ZA* zoledronic acid, *Dmab* denosumab. **a** The mean SUVs of the ROIs at the cervical vertebrae. **b** The mean SUVs of the ROIs at the thoracic vertebrae

differences between the Dmab and Control groups were observed at any of the sites (Table 2, Fig. 2). The inter-observer and intra-observer reliability data of each SUV measurement are provided in Table 2. The ICC range of the inter-observer analysis was 0.748–0.949, which indicates substantial to almost perfect reliability. The ICC range of the intra-observer reliability analysis was 0.869–0.987, which also indicates almost perfect reliability.

Discussion

The normal mandibular bone in the ZA group and the femur in both the ZA group and Dmab group did not exhibit suppressed bone metabolism. In the ZA group, the bone metabolism was suppressed at the cervical vertebrae compared to the healthy controls, and the bone metabolism at the thoracic vertebrae of the ZA group was also suppressed compared to both the Dmab and Control groups; in the Dmab group, no significant difference compared to the controls was observed. Our hypothesis that ZA and Dmab equally suppress bone remodeling of the normal mandible was, therefore, not confirmed.

Ristow et al. reported that in 45 female patients with breast cancer, the bone turnover of the mandible and femur was not significantly altered after treatment with both BP and Dmab [20]. This is consistent with our present findings. We speculate that changes in the bone metabolism of the mandible and femur depend on external forces due to mastication, walking and posture, in addition to changes due to aging, nutritional intake, and the presence or absence of teeth on the mandible. However, it is unclear why the bone metabolism of the jaw and femur was not suppressed by ZA or Dmab. The inhibition of bone remodeling may not affect the pathogeneses of AFF and MRONJ.

Zoledronic acid is one of several BP formulations used clinically. The osteoclasts absorb and take in the bone together with the BP that is bound to the bone [21]. Osteoclasts that have taken up BP undergo apoptosis [22]. As a result, the osteoclasts are unable to resorb bone. The induction of osteoclast apoptosis can reduce SREs associated with bone metastasis [23]. Bisphosphonates rapidly bind to bone by chelating calcium ions on the surfaces of hydroxyapatite [24]. After bone binds to a BP, the BP is released when the bone on which the BP is deposited is resorbed by osteoclasts. The half-life of a BP in bone is thus very long, varying from 1 to 10 years, depending greatly on the rate of bone turnover [25]. Bisphosphonates also bind preferentially to bones with high turnover, and the distribution of a BP at bone is not homogeneous; the BP uptake is greater in trabecular bone compared to cortical bone due to the greater blood flow, surface area, and bone turnover in trabecular bone [25].

Bone is composed of cortical bone and cancellous bone, with cortical bone accounting for 75% and cancellous bone for 25%. Cortical and cancellous bone differ in terms of bone metabolism, with 4% cortical bone turnover and 25% cancellous bone turnover per year [26]. The composition of the jawbone has been reported to have a cortical bone area of 44–54.2%, but since the femoral neck accounts for 17.9%, the proportion of cancellous bone in the jawbone is lower than in other parts [27]. In contrast, the spine is mainly cancellous bone. We speculate that our present finding was obtained, because the effect of the patients' treatment with a BP on bone metabolism suppression in the vertebrae was strong.

Denosumab is an anti-RANKL antibody and thus a targeted drug that targets RANKL. It binds to the produced RANKL and prevents RANK on osteoclast precursors from binding to RANKL [21]. As a result, osteoclast precursors die without reaching mature osteoclasts. Denosumab

prevents fractures and suppresses the expression of SREs by inhibiting the differentiation into mature osteoclasts [23]. The different mechanisms of action of the inhibition of bone resorption between Dmab and ZA may thus explain why the Dmab group's results were not significantly different from those of the Control group.

^{18}F-Fluoride is a PET tracer for bone. ^{18}F-ions accumulate in bone tissue after the hydroxyl groups of hydroxyapatite produced in the remodeling process are replaced with ^{18}F-ions and are bound [28]. The amount of accumulation depends on the local blood flow and the remodeling activity at the bone metastasis site [29]. PET with ^{18}F-fluoride has many advantages over traditional bone scintigraphy. The sensitivity and specificity are high and images are produced more quickly (within 1 h after injection, as the acquisition time is short) [18]. In addition, the correlation by a CT examination allows us to pinpoint the anatomical location of lesions, increasing the research specificity [30]. Our present examination method thus appears to be more sensitive and more specific than previous reports about the response of bone metabolism to antiresorptive agents using bone scintigraphy [20].

The uptake of F-ions into normal bone with ^{18}F-NaF-PET is predominant in axial bone [31], and the SUV is reported to be different at each site. The lumbar spine, thoracic spine, and cervical spine have higher SUVs than the femoral head, and parietal and humeral bones have lower SUVs [32]. The significant differences in the SUVs of the present Control group are consistent with that report [32].

Our study has several limitations. We did not determine the presence or absence of teeth, vital or nonvital teeth, masticatory ability, walking ability, or nutritional intake, all of which might affect bone metabolism. Moreover, due to the small sample size, our results should be validated by further studies. The values obtained before and after medical treatment in the same sample should also be acquired in a future investigation.

Here, using the SUV obtained by ^{18}F-NaF-PET, we report for the first time that the effects of BP and Dmab on normal bone are different. The decreased uptake of ^{18}F-NaF in the ZA group could be explained by the inhibition of osteoblastic activity following the suppression of osteoclastic activity caused by this BP [33–35]. However, we were unable to find any studies that performed ^{18}F-NaF-PET imaging after Dmab treatment. It is necessary that we focus on the mechanism of ^{18}F-NaF accumulation for Dmab.

Our results revealed that bone metabolism was characterized by its location. The remodeling of mandibular bone was not suppressed by treatment with the antiresorptive agents. It is likely that the different mechanisms of action of the inhibition of bone resorption between bisphosphonates and denosumab caused the differences in their effects on the metabolism of normal bone.

Funding This study did not receive any funding.

Declarations

Conflict of interest The authors declare that they have no conflict of interest.

Ethical approval All procedures performed in studies involving human participants were in accordance with the ethical standards of the institutional and/or national research committee (the Kagawa University Ethical Committee (2020-#122)) and with the 1964 Helsinki Declaration and its later amendments or comparable ethical standards.

Informed consent Informed consent was obtained from all individual participants included in the study.

References

1. Coleman RE. Metastatic bone disease: clinical features, pathophysiology and treatment strategies. Cancer Treat Rev. 2001;27:165–76.
2. Lipton A. Management of bone metastases in breast cancer. Curr Treat Options Oncol. 2005;6:161–71.
3. Coleman RE, Rubens RD. The clinical course of bone metastases from breast cancer. Br J Cancer. 1987;55:61–6.
4. O'Reilly SM, Richards MA, Rubens RD. Liver metastases from breast cancer: the relationship between clinical, biochemical and pathological features and survival. Eur J Cancer (Oxford, England: 1990). 1990;26:574–7.
5. Wu S, Dahut WL, Gulley JL. The use of bisphosphonates in cancer patients. Acta Oncol. 2007;46:581–91.
6. McClung M, Harris ST, Miller PD, et al. Bisphosphonate therapy for osteoporosis: benefits, risks, and drug holiday. Am J Med. 2013;126:13–20.
7. Ruggiero SL, Dodson TB, Fantasia J, et al. American association of oral and maxillofacial surgeons position paper on medication-related osteonecrosis of the jaw - 2014 update. J Oral Maxillofac Surg. 2014;72:1938–56.
8. Khan AA, Morrison A, Hanley DA, et al. Diagnosis and management of osteonecrosis of the jaw: a systematic review and international consensus. J Bone Miner Res. 2015;30:3–23.
9. Takahashi M, Ozaki Y, Kizawa R, et al. Atypical femoral fracture in patients with bone metastasis receiving denosumab therapy: a retrospective study and systematic review. BMC Cancer. 2019;19:980.
10. Limones A, Sáez-Alcaide LM, Díaz-Parreño SA, et al. Medication-related osteonecrosis of the jaws (MRONJ) in cancer patients treated with denosumab VS. zoledronic acid: a systematic review and meta-analysis. Med Oral Patologia Oral y Cirugia Bucal. 2020;25:e326–36.
11. Lockwood M, Banderudrappagari R, Suva LJ, Makhoul I. Atypical femoral fractures from bisphosphonate in cancer patients—review. J Bone Oncol. 2019;18:100259.
12. Shane E, Burr D, Abrahamsen B, et al. Atypical subtrochanteric and diaphyseal femoral fractures: second report of a task force of the American Society for Bone and Mineral Research. J Bone Miner Res. 2014;29:1–23.

13. Gong X, Yu W, Zhao H, Su J, Sheng Q. Skeletal site-specific effects of zoledronate on in vivo bone remodeling and in vitro BMSCs Osteogenic Activity. Sci Rep. 2017;7:36129.
14. Chang J, Hakam AE, McCauley LK. Current understanding of the pathophysiology of osteonecrosis of the jaw. Curr Osteoporos Rep. 2018;16:584–95.
15. Blau M, Nagler W, Bender MA. Fluorine-18: a new isotope for bone scanning. J Nucl Med. 1962;3:332–4.
16. Li Y, Schiepers C, Lake R, Dadparvar S, Berenji GR. Clinical utility of 18F-fluoride PET/CT in benign and malignant bone diseases. Bone. 2012;50:128–39.
17. Even-Sapir E, Mishani E, Flusser G, Metser U. 18F-fluoride positron emission tomography and positron emission tomography/computed tomography. Semin Nucl Med. 2007;37:462–9.
18. Grant FD, Fahey FH, Packard AB, et al. Skeletal PET with 18F-fluoride: applying new technology to an old tracer. J Nucl Med. 2008;49:68–78.
19. Langsteger W, Rezaee A, Pirich C, Beheshti M. (18)F-NaF-PET/CT and (99m)Tc-MDP bone scintigraphy in the detection of bone metastases in prostate cancer. Semin Nucl Med. 2016;46:491–501.
20. Ristow O, Gerngroß C, Schwaiger M, et al. Effect of antiresorptive drugs on bony turnover in the jaw: denosumab compared with bisphosphonates. Br J Oral Maxillofac Surg. 2014;52:308–13.
21. Baron R, Ferrari S, Russell RGG. Denosumab and bisphosphonates: different mechanisms of action and effects. Bone. 2011;48:677–92.
22. Plotkin LI, Bivi N, Bellido T. A bisphosphonate that does not affect osteoclasts prevents osteoblast and osteocyte apoptosis and the loss of bone strength induced by glucocorticoids in mice. Bone. 2011;49:122–7.
23. Rosen LS, Gordon D, Tchekmedyian S, et al. Zoledronic acid versus placebo in the treatment of skeletal metastases in patients with lung cancer and other solid tumors: a phase III, double-blind, randomized trial—the Zoledronic Acid Lung Cancer and Other Solid Tumors Study Group. J Clin Oncol. 2003;21:3150–7.
24. Cole L, Vargo-Gogola T, Roeder R. Targeted delivery to bone and mineral deposits using bisphosphonate ligands. Adv Drug Deliv Rev. 2015;99:12.
25. Lin JH. Bisphosphonates: a review of their pharmacokinetic properties. Bone. 1996;18:75–85.
26. Manolagas SC. Birth and death of bone cells: basic regulatory mechanisms and implications for the pathogenesis and treatment of osteoporosis*. Endocr Rev. 2000;21:115–37.
27. Matsuura T, Mizumachi E, Katafuchi M, et al. Sex-related differences in cortical and trabecular bone quantities at the mandibular molar. J Hard Tissue Biol. 2014;23:267–74.
28. Blau M, Ganatra R, Bender MA. 18F-fluoride for bone imaging. Semin Nucl Med. 1972;2:31–7.
29. Cook GJ, Fogelman I. Detection of bone metastases in cancer patients by 18F-fluoride and 18F-fluorodeoxyglucose positron emission tomography. Q J Nucl Med. 2001;45:47–52.
30. Bortot DC, Amorim BJ, Oki GC, et al. ^{18}F-Fluoride PET/CT is highly effective for excluding bone metastases even in patients with equivocal bone scintigraphy. Eur J Nucl Med Mol Imaging. 2012;39:1730–6.
31. Sarikaya I, Elgazzar AH, Sarikaya A, Alfeeli M. Normal bone and soft tissue distribution of fluorine-18-sodium fluoride and artifacts on ^{18}F-NaF PET/CT bone scan: a pictorial review. Nucl Med Commun. 2017;38:810–9.
32. Win AZ, Aparici CM. Normal SUV values measured from NaF18-PET/CT bone scan studies. PLoS ONE. 2014;9:e108429-e.
33. Raje N, Woo S-B, Hande K, et al. Clinical, radiographic, and biochemical characterization of multiple myeloma patients with osteonecrosis of the jaw. Clin Cancer Res. 2008;14:2387–95.
34. Arce K, Assael LA, Weissman JL, Markiewicz MR. Imaging findings in bisphosphonate-related osteonecrosis of jaws. J Oral Maxillofac Surg. 2009;67:75–84.
35. Wilde F, Steinhoff K, Frerich B, et al. Positron-emission tomography imaging in the diagnosis of bisphosphonate-related osteonecrosis of the jaw. Oral Surg Oral Med Oral Pathol Oral Radiol Endodontol. 2009;107:412–9.